Recruitment abundance index of immature Pacific bluefin tuna, derived from real-time monitoring survey data of troll fisheries

Ko Fujioka, Saki Asai, Yohei Tsukahara,

Hiromu Fukuda and Shuya Nakatsuka

Highly Migratory Resources Division, Fisheries Resources Institute,

Japan Fisheries Research and Education Agency

5-7-1, Orido, Shimizu, Shizuoka 424-8633, JAPAN

March 2023

Working document submitted to the ISC Pacific bluefin tuna Working Group, International Scientific Committee for Tuna and Tuna-Like Species in the North Pacific Ocean (ISC), from 21 to 24 March 2023, Tokyo, Japan.

Summary

In this study, we provided a recruitment abundance index of Pacific bluefin tuna using real-time troll monitoring (RTM) data instead of a traditional index based on sales slip data. The standardized CPUE based on RTM data was calculated by Vector Autoregressive Spatio-Temporal (VAST) model which is a delta-generalized linear mixed model that separately calculates the encounter probability and the positive catch rate, as in Fujioka et al. (2021, 2022). Estimated index for 2011-2022 showed a similar trend to the index based on traditional sales slip data for the overlap period (2011-2016). In addition, the IQ-Independent scientific survey by monthly chartering RTM vessels began from the 2021 fishing year (Fujioka et al., 2022). The estimated indices with and without this chartered RTM data were almost identical, and CV values were small when including the chartered RTM data. Therefore, the recruitment indices for two time periods presented in this study, 2011-2022 (the full RTM period) and 2017-2022 (the period of tightened fishing regulations), would be candidates for input into the stock assessment model in the next assessment.

Introduction

The recruitment abundance index (i.e. standardized CPUE) based on troll fishery data is one of the most important input data for the Pacific bluefin tuna (PBF) stock assessment. However, Nishikawa et al. (2021) reviewed the fishery data for estimating abundance index and reported that calculated index might be negatively biased after 2016 due to the changes in fishery operation (increasing of the live release at sea) responding to management measures (e.g. minimum size limitation and substantial individual quota management) and thus can not be used for the stock assessment conducted in 2022. Therefore, PBFWG needs to explore/develop a recruitment abundance index using alternative data to sales slip data.

In the last stock assessment (ISC 2022), the recruitments from 2017 to 2020 were estimated based on mainly the assumed stock-recruitment relationship (SRR) since there were limited recruitment information in the base-case model, and consequently those were estimated as no deviations from the SRR. Additionally, real-time troll monitoring (RTM) survey data was also used in the sensitivity analysis of the assessment and projections as an alternative index to traditional troll index to seek the potential effect of the alternative index on the results of the current base case as well as the management advice based on that. The performance of the estimated index using RTM data was reported as similar to traditional troll CPUE when those two indices were overlapped (Fukuda et al., 2021). For the upcoming full stock assessment in 2024, it is desirable to input the reliable latest recruitment information into the model for the stock analysis to make the advice with consideration about the most recent recruitment figure.

Because of troll sales slip data was strongly affected by fishing regulations, the RTM survey index was submitted to the PBFWG (Fujioka et al., 2021, 2022). The RTM data provides geographic information on operations by vessels, allowing us to aggregate catch and effort data into a detailed latitude-longitude grids. The advantage of the monitoring data is that live release data and zero-catch operations can be obtained in a spatiotemporally fine-grained and timely manner (Tsukahara et al., 2019). However, as fishing regulations are tightened, even data from monitoring survey became sparse by fishing suspensions when fishing quotas (e.g. IQ; individual quota, local fisheries association based quota or area based quota, prefecture based quota) were exceeded throughout the fishing season. Therefore, in order to properly understand the recent trends of recruitment, Japan Fisheries Research and Education Agency (FRA) has started a scientific survey using charter operations of RTM vessels from the 2021 fishing year, adding to conventional RTM from 2011 by commercial vessels. The chartered troll RTM operated in the same time and space (operating hours and area) as conventional RTM, are allowed to conduct IQ-independent research fishing. Fourteen RTM vessels were chartered to conduct survey operation for 10 days per four months from November to February with at least one operation in each month (Fujioka et al., 2022). A comparison of the spatio-temporal operational patterns of conventional RTM and charter RTM confirmed that their combined data interpolate each other’s spatio-temporal strata, although it was from a single year of analysis (Fujioka et al., 2022).

In this working paper, we attempted to estimate recruitment indices for the entire period of troll RTM data collection from 2011 to 2022 and for the period of tightened fishing regulations from 2017 to 2022. For the period of 2017-2022, two recruitment indices are presented: based on i) the full data set using conventional and chartered RTM data, and ii) only conventional RTM data, to identify differences in trends due to the use of some different data. We explored area-weighted recruitment index using the spatio-temporal delta-generalized liner mixed modelling method (VAST: Vector Autoregressive Spatio-Temporal) (Thorson, 2019) with the expectation of reducing bias due to reduced sampling area caused by fishing regulations, according to the similar approach to Fujioka et al. (2021, 2022).

Methods

Data collection and summary

Data from 14 RTM vessels, which targeted for age-0 PBF (i.e. 40-60 cm fork length) during the winter season (November to following February) in the East China Sea (ECS), have been collected since 2011 fishing year. The RTM data were collected in the same season and area as the traditional troll indices (sales slip basis) which represents the abundance of juvenile PBF born in both main spawning grounds in the North Western Pacific Ocean and the Sea of Japan. Locations of fishing port for those RTM vessels are shown in Figure 1. The number of RTM vessels increased to 14 vessels up to date, and operational data were collected from 7 to 14 vessels each fishing year (Figure 2). This paper updates the operational data by 14 vessels for the analysis period of 2011-2022 (Table 1). Since 2021 fishing year, in addition to conventional RTM, those conventional 14 RTM vessels were chartered for 10 days from November through February with at least one operation in each month to secure operations in the monitoring period, namely chartered RTM. They can operate independently with IQ as the catch from chartered operations were reported as part of the national government authorized FRA survey quota. Unless otherwise noted, the data from chartered RTM is included in the analysis.

RTM vessels are equipped with the GPS receiver and numeric keypad to input species and number of fish caught at the fishing location. The GPS data is recorded at intervals of 1 second during all trips. The vessel velocity can be estimated by the moving distance based on the GPS data. The estimated velocity was smoothed by the trimmed mean to exclude the obvious outlier due to the unsettled GPS data. These trace of fishing behavior and catch position can be used to estimate more precise efforts in an operation, i.e., actual operation time, than the catch per day used for sales slip data. PBF operation was defined as continuous vessel's velocity in the range of 2-7knot for more than 30 minutes. The PBF catch and effort (residence time in minutes) data were aggregated in a 0.1×0.1 degree latitude/longitude grids and formatted into the following data; vessel name, year, month, day, latitude, longitude, catch, effort.

Data was carefully reviewed and any operations that were not clearly PBF operations based on the vessel's track and location records was removed by expert judgement. This is because fishermen may operate targeting other fish species due to changes in the catchability of PBF and/or demand for farming depending on year and season. We also excluded data that had obvious errors in the numeric keypad entry on board (e.g., more than 500 catches in one operation). Also, data in the northeastern part of Tsushima (latitude >34.5, longitude >129.2) was excluded (38 grids) because it was a unique fishing ground only for the 2011 fishing year (Fujioka et al. 2021). This kind of data in rarely sampled area may affect the estimation of spatial effect of whole time series by the nature of VAST model for sharing information over space and time.

The spatial distribution of RTM operations by year is shown in Figure 3. Histograms of fishing effort (in minutes) and PBF catch records from 2011 to 2022 are shown in Figure 4. For the 0.1 degree grid aggregated data, the mean and standard deviation for fishing effort was 102.2 ± 104.8 minutes, ranging from 5 to 735 minutes. The mean and standard deviation of PBF catch was 3.3 ± 10.4 with a range of 0 to 284. For the entire period (2011-2022), the zero-catch rate operation was 67%, the positive catch rate was 33%, and the coefficient of variation of PBF catch (S.D./Mean) was 3.20. Nominal CPUE for each month and fishing year is shown in Figure 5. The latest 2022 data is presented in Table 2, and showing the spatio-temporal (area and monthly) differences between conventional and charter RTM operations (Fig. 6).

Vector Autoregressive Spatio-Temporal (VAST) model

VAST is a delta-generalized linear mixed model that separately calculates the encounter probability and the positive catch rate, and is available from the R package "VAST" version 3.8.0 on the website (https://github.com/James-Thorson-NOAA/VAST) (Thorson, 2019). In our study, the encounter probability (*p*) at observation *i* was modeled using a logit-linked linear predictor, and the positive catch rate (*r*) at observation i was modeled using a log-linked linear predictor, as in the following equation:

(1) $\text{logit}(p_i) = \beta_1(t_i) + L_{\omega 1}\omega_1(s_i) + L_{\varepsilon 1}\varepsilon_1(s_i, t_i) + \zeta_1(s_i, m_i) + L_{\eta 1}\eta_1(v_i)$

(2) $\log(r_i) = \beta_2(t_i) + L_{\omega 2}\omega_2(s_i) + L_{\varepsilon 2}\varepsilon_2(s_i, t_i) + \zeta_2(s_i, m_i) + L_{\eta 2}\eta_2(v_i)$

where $\beta(t_i)$ is the intercept in year t_i, $\omega(s_i)$ is the time-invariant spatial variations at location s_i, $\varepsilon(s_i, t_i)$ is the time-varying spatio-temporal variations at location s_i in year t_i, $\zeta(s_i, m_i)$ is the s_i month effect m_i as a catchability covariate which is either spatially varying at location at s_i

or spatially constant by configuration and $\eta(v_i)$ is the effect of vessel v_i as a factor of overdispersion, and L_ω, L_ε and L_η are the scaling coefficients of the random effect distributions (Fujioka et al., 2021, 2022).

The probability of the density c is specified in this study as follows for a zero-inflated Poisson distribution:

$$(3)\ \Pr(c_i = c) = \begin{cases} 1 - p_i & \text{if } c = 0 \\ p_i \times ZeroInflated\ Poisson(c_i | \log(r_i), \sigma^2) & \text{if } c > 0 \end{cases}$$

where σ^2 is a dispersion parameter.

Then, the abundance index was predicted using an area-weighted approach, which calculates total abundance as a weighted sum of the estimated densities in a pre-defined spatial domain of knots. The number of knots was set equal to the number of observation locations (214 knots for 2011-2022).

Regarding the configuration of spatial structure with Gaussian Random Markov field (GRMR), this analysis used the anisotropic estimation of correlation, which estimate two different parameters for the correlation of two independent directions. In terms of temporal configuration, there is no assumption of correlated structure both year effect itself and spatio-temporal variation because the recruitment strength was highly variable over years based on the PBF assessment result.

Results and Discussion

This study provides updated data on RTM of age-0 PBF in the ECS (Fig. 1) during winter based on twelve years (2011-2022) including the fishing regulation period. Operational data of RTM survey were obtained over 96-498 operational days with ranging 54-214 latitude/longitude grids from up to 14 vessels in each year (Table 1, Fig. 2). Since 2021 fishing year, IQ-independent charter RTM surveys were initiated to ensure sufficient operations in each spatial and temporal stratum. Fujioka et al. (2021) reported that two types of RTM data sets (chartered operation data and non-chartered operation data) for 2021 were found to be useful that complement each other's spatio-temporal information. The operational patterns of conventional RTM and chartered RTM in the 2022 were also examined with a focus on the ratio of spatial grids to each other (Table 2, Figure 6). The results showed that the ratio of the number of spatial grids in the chartered survey to the number of spatial grids in the conventional survey was sufficiently high (99.1% of the monthly total). In other words, the monthly spatial distribution of the chartered survey improves the data set for estimating recruitment abundance index.

Additionally, in February 2022, conventional RTM was not conducted around Tsushima (Figure 6(b), bottom light) because fishermen reported that the PBF was passing southward (i.e. Goto Is.) due to low sea surface temperature (15.3°C). In this situation, conventional RTM could not provide information, but the charter RTM was initiated to provide additional fishery information (Fig.6 (c) bottom right) even for zero-catch operations. This demonstrated the importance/advantage of the charter RTM survey, which covers the spatio-temporal scale throughout the fishing season.

Area-weighted standardized CPUEs for the entire period of 2011-2022 were estimated from spatio-temporal model analysis using the RTM vessel's data. The full model (Case 1) that assumed spatial and spatio-temporal effects, month effect as catchability covariate which was spatially varying for each of encounter probability and positive catch rate was judged to be the best model in terms of the AIC criteria (Table 3-1). The model converged successfully and the final gradients on each parameter were well below (Table 4-1). Quantile diagnostics of these models also showed no considerable negative signs in the standardization (Fig. 12-1). The result of distance of 10% correlation of both encounter probability and positive catch rate was estimated as anisotropic shapes with approximately 30-60km of latitude axis mainly from south to north in each period of time (Fig. 8-1), so that the estimation in certain grids have some impacts on estimation in the approximately 3-6 grids away from there in 0.1 by 0.1 degree grid. This means that spatial correlation seems to be limited for availability of age-0 PBF. A longer period of data accumulation is needed to clarify the pattern of relationship between the PBF biomass distribution and the estimated biomass (Fig. 9-1, 10-1).

Similar to the period of 2011-2022, for the period of 2017-2022, the full model (Case 1) was selected as the best model (Table 3-2). Also for the data without chartered RTM operation, the full model (Case 1) was determined to be the best (Table 3-3). The both models converged successfully, and the final gradients for each parameter were satisfactory for this 2017-2022 dataset, respectively (Table 4-2, 4-3). Quantile diagnostics of these models also showed no considerable negative signs in the standardization each data period (Fig. 12-2). Decorrelation distance for different directions relative to encounter probability and positive catch rate are shown in Figure 8-2, and the patterns of center of the PBF biomass distribution in Figure 9-2, respectively. Changes in the center of the PBF biomass distribution in the east-west and north-south directions did not show a clear pattern with the estimated biomass in this short period (Fig. 9-2).

The comparison of the standardized indices by VAST (Case 1 for 2011-2022, Case 1 for 2017-2022 and Case 1 for 2017-2022 without chartered RTM data) and traditional GLM index is shown in Figure 13. Trends for the three indices estimated in this study after 2016 were generally similar. The difference in the scaled indices for these higher periods (2017-2018 and 2021-2022) is considered due to the different scaling periods of data set between 2011-2022 and 2017-2022. It should also be emphasized that the estimated indices for 2011-2022 were quite similar to the traditional sales slip index throughout the overlapping period (2011-2016). If the PBFWG requests recruitment indicator before 2017 period in the stock assessment analysis, RTM indices would be available for the longer time series (2011-2022) as well as for the strict catch regulation period (2017-2022). The latest high index values in 2021-2022 of RTM indices were robust whichever using chartered RTM data or not, and the index with the chartered RTM data showed smaller CV than that without the chartered RTM data (Fig. 11). It suggested that adding to chartered RTM data to conventional RTM data are considered reasonable.

In conclusion, our estimated RTM index has a better use of available information than the traditional troll CPUE index of sales slip basis while showing a similar trend, and can be switched to an earlier year (i.e. 2011), which would inform the stock assessment model about the relative strength of recruitment at a higher resolution.

References

Fukuda, H., Fujioka, K., Tsukahara, Y., Nishikawa, K. and Nakatsuka, S. 2021. Reinforcement of Japanese PBF recruitment monitoring program. ISC/21/PBFWG-1/06.

Fujioka, K., Tsukahara, Y., Asai, S., Nishikawa, K., Fukuda, H. and Nakatsuka, S. 2021. Estimation of recruitment index of Pacific bluefin tuna based on real-time troll monitoring survey data using Vector Autoregressive Spatio-Temporal (VAST) model analysis. ISC/21/PBFWG-02/03.

Fujioka, K., Tsukahara, Y., Asai, S., Fukuda, H. and Nakatsuka, S. 2022. Update of estimated recruitment index of Pacific bluefin tuna based on real-time troll monitoring survey data, added IQ-independent scientific survey data for 2021. ISC/22/PBFWG-02/01.

ISC 2022. Report of the Pacific bluefin tuna working group intersessional workshop. ISC/22/ANNEX/06.

Nishikawa, K., Tsukahara, Y., Fujioka, K., Fukuda, H. and Nakatsuka, S. 2021. Update of age-0 PBF index based on catch per unit effort data from Japanese troll fishery and its associated issues. ISC/21/PFWG-1/05.

Thorson, JT. 2019. Guidance for decisions using the Vector Autoregressive Spatio-Temporal (VAST) package in stock, ecosystem, habitat and climate assessments. *Fish. Res.* 210: 143-161.

Tsukahara, Y. and Chiba, K. 2019. Real-time recruitment monitoring for Pacific bluefin tuna using CPUE for troll vessels: Update up to 2018 fishing year. ISC/19/PBFWG-1/04.

Table 1 (a) Total number of efforts (in days) and (b) number of latitude/longitude grids (in 0.1 grid units) by 7-14 real-time troll monitoring vessels per month from 2011 to 2022 fishing year.

a)	Total number of troll operations (days)											
	2011	2012	2013	2014	2015	2016	2017	2018	2019	2020	2021	2022
November	31	67	27	42	113	64	57	67	35	30	90	49
December	99	93	67	71	163	53	39	112	88	49	165	76
January	58	58	110	120	107	80	0	132	176	30	114	99
February	74	0	90	20	115	74	0	120	107	23	121	82
Total	262	218	294	253	498	271	96	431	406	132	490	306

b)	Total number of troll operations (grids)											
	2011	2012	2013	2014	2015	2016	2017	2018	2019	2020	2021	2022
November	22	30	29	27	43	31	24	31	25	25	48	26
December	50	64	40	54	75	40	30	28	30	36	69	46
January	68	68	71	91	42	38	0	62	30	32	59	44
February	64	0	63	36	52	62	0	63	44	29	38	49
Total	204	162	203	208	212	171	54	184	129	122	214	165

Table 2 Monthly effort (in days) and grid (in 0.1 grid units) of conventional real-time monitoring and chartered real-time monitoring by 14 troll vessels in the 2022 fishing year. Both monitoring surveys were conducted by the same 14 troll vessels. *See* Figure 6 for the difference in the monthly spatial distribution of operations for both monitoring vessels.

	Total operation		Conventional		Charter		Ratio of chater to conventional	
	days	grids	days	grids	days	grids	days (%)	grids (%)
November	49	26	32	21	17	22	53.1	104.8
December	76	46	31	20	45	39	145.2	195.0
January	99	44	57	37	42	20	73.7	54.1
February	82	49	49	36	33	32	67.3	88.9
Total	306	165	169	114	137	113	81.1	99.1

Table 3-1 Combinations of explanatory variables for encounter probability (*p*) and positive catch (*r*) in a delta model and the values of Akaike information criterion (AIC) for the period 2011-2022. Delta AIC indicates the difference between the case 1 model with the lowest AIC. Blank means no convergence.

Case	Model for *p*	Model for *r*	AIC	*Δ* AIC
1	**Yr + Station + Yr:Station + Month(spatially varying) + Vessel**	**Yr + Station + Yr:Station + Month(spatially varying) + Vessel**	**58661**	**0**
2	Yr + Station + Yr:Station + Month(spatially varying) + Vessel	Yr + Station + Yr:Station + Month(spatially constant) + Vessel	60582	1921
3	Yr + Station + Yr:Station + Month(spatially constant) + Vessel	Yr + Station + Yr:Station + Month(spatially varying) + Vessel	58676	15
4	Yr + Station + Yr:Station + Month(spatially constant) + Vessel	Yr + Station + Yr:Station + Month(spatially constant) + Vessel	60626	1965
5	Yr + Station + Yr:Station + Month(spatially varying)	Yr + Station + Yr:Station + Month(spatially varying)	60295	1634
6	Yr + Station + Yr:Station + Month(spatially varying)	Yr + Station + Yr:Station + Month(spatially constant)	62108	3447
7	Yr + Station + Yr:Station + Month(spatially constant)	Yr + Station + Yr:Station + Month(spatially varying)	60309	1648

Table 3-2 Continuing with the dataset for the period 2017-2022. Delta AIC indicates the difference between the case 1 model with the lowest AIC. Blank means no convergence.

Case	Model for *p*	Model for *r*	AIC	*Δ* AIC
1	**Yr + Station + Yr:Station + Month(spatially varying) + Vessel**	**Yr + Station + Yr:Station + Month(spatially varying) + Vessel**	**32314**	**0**
2	Yr + Station + Yr:Station + Month(spatially varying) + Vessel	Yr + Station + Yr:Station + Month(spatially constant) + Vessel	33764	1450
3	Yr + Station + Yr:Station + Month(spatially constant) + Vessel	Yr + Station + Yr:Station + Month(spatially varying) + Vessel		
4	Yr + Station + Yr:Station + Month(spatially constant) + Vessel	Yr + Station + Yr:Station + Month(spatially constant) + Vessel	33824	1510
5	Yr + Station + Yr:Station + Month(spatially varying)	Yr + Station + Yr:Station + Month(spatially varying)		
6	Yr + Station + Yr:Station + Month(spatially varying)	Yr + Station + Yr:Station + Month(spatially constant)	34950	2636
7	Yr + Station + Yr:Station + Month(spatially constant)	Yr + Station + Yr:Station + Month(spatially varying)		

Table 3-3 Continuing with the dataset without chartered vessels for the period 2017-2022. Delta AIC indicates the difference between the case 1 model with the lowest AIC. Blank means no convergence.

Case	Model for *p*	Model for *r*	AIC	*Δ* AIC
1	**Yr + Station + Yr:Station + Month(spatially varying) + Vessel**	**Yr + Station + Yr:Station + Month(spatially varying) + Vessel**	**23962**	**0**
2	Yr + Station + Yr:Station + Month(spatially varying) + Vessel	Yr + Station + Yr:Station + Month(spatially constant) + Vessel	25012	1050
3	Yr + Station + Yr:Station + Month(spatially constant) + Vessel	Yr + Station + Yr:Station + Month(spatially varying) + Vessel	23985	23
4	Yr + Station + Yr:Station + Month(spatially constant) + Vessel	Yr + Station + Yr:Station + Month(spatially constant) + Vessel	25075	1113
5	Yr + Station + Yr:Station + Month(spatially varying)	Yr + Station + Yr:Station + Month(spatially varying)	24788	826
6	Yr + Station + Yr:Station + Month(spatially varying)	Yr + Station + Yr:Station + Month(spatially constant)	25737	1775
7	Yr + Station + Yr:Station + Month(spatially constant)	Yr + Station + Yr:Station + Month(spatially varying)	24802	840

Table 4-1 Initial and final condition of each parameter related to explanatory variables in the 2011-2022 period. The list of parameters is as follows: beta; intercept for 1st or 2nd linear predictor (1st; encounter probability, 2nd; positive catch rate) each fishing year (2011-2020), L_eta; overdispersion factors (vessels) for 1st or 2nd linear predictor, L_omega; spatial factors for 1st or 2nd linear predictor L_epsilon; spatio-temporal factors for 1st or 2nd linear predictor, logkappa; decorrelation rate for 1st or 2nd linear predictor, log_sigmaPh; conditional variance between each month for intercepts of 1st linear predictor

Parameter	Starting value	Lower boundary	Maximum likelihood estimation	Upper boundary	Final gradient
ln_H_input	-0.17921	-5	-0.17921	5	2.51E-10
ln_H_input	0.08261	-5	0.08261	5	7.86E-10
beta1_ft_2011	-0.58020	-Inf	-0.58004	Inf	2.39E-10
beta1_ft_2012	-0.97118	-Inf	-0.97105	Inf	-2.54E-10
beta1_ft_2013	-0.47775	-Inf	-0.47760	Inf	-2.34E-10
beta1_ft_2014	-0.99076	-Inf	-0.99062	Inf	-9.03E-11
beta1_ft_2015	-0.64699	-Inf	-0.64684	Inf	2.84E-10
beta1_ft_2016	0.49975	-Inf	0.49992	Inf	-1.64E-09
beta1_ft_2017	0.80420	-Inf	0.80432	Inf	-2.30E-09
beta1_ft_2018	-0.23329	-Inf	-0.23312	Inf	2.22E-10
beta1_ft_2019	-0.93983	-Inf	-0.93967	Inf	-2.34E-10
beta1_ft_2020	-0.57015	-Inf	-0.56997	Inf	-5.29E-10
beta1_ft_2021	0.72781	-Inf	0.72798	Inf	3.45E-11
beta1_ft_2022	0.85593	-Inf	0.85611	Inf	5.24E-10
L_eta1_z	0.61650	-Inf	0.61650	Inf	-6.24E-08
L_omega1_z	-1.03730	-Inf	-1.03731	Inf	1.16E-07
L_epsilon1_z	-0.76891	-Inf	-0.76892	Inf	3.53E-08
logkappa1	-2.81363	-4.790245	-2.81362	-1.17374	1.19E-07
log_sigmaPhi1_k	-0.72376	-Inf	-0.72380	Inf	9.83E-09
log_sigmaPhi1_k	-0.55383	-Inf	-0.55383	Inf	-3.61E-09
log_sigmaPhi1_k	-0.09845	-Inf	-0.09845	Inf	-2.08E-09
beta2_ft_2011	-3.47247	-Inf	-3.47249	Inf	4.52E-10
beta2_ft_2012	-3.56226	-Inf	-3.56228	Inf	1.90E-10
beta2_ft_2013	-3.03112	-Inf	-3.03112	Inf	-2.93E-10
beta2_ft_2014	-4.34369	-Inf	-4.34370	Inf	-3.70E-10
beta2_ft_2015	-3.94072	-Inf	-3.94072	Inf	-5.92E-10
beta2_ft_2016	-3.02413	-Inf	-3.02414	Inf	2.80E-09
beta2_ft_2017	-2.87330	-Inf	-2.87333	Inf	9.27E-10
beta2_ft_2018	-2.93373	-Inf	-2.93374	Inf	7.13E-12
beta2_ft_2019	-3.55722	-Inf	-3.55726	Inf	-5.72E-11
beta2_ft_2020	-3.49707	-Inf	-3.49711	Inf	2.03E-09
beta2_ft_2021	-2.70767	-Inf	-2.70767	Inf	-6.69E-10
beta2_ft_2022	-3.20693	-Inf	-3.20693	Inf	-5.29E-10
L_eta2_z	-0.33773	-Inf	-0.33773	Inf	4.81E-09
L_omega2_z	-0.28379	-Inf	-0.28379	Inf	1.23E-08
L_epsilon2_z	0.83860	-Inf	0.83860	Inf	-4.29E-08
logkappa2	-2.05444	-4.790245	-2.05444	-1.17374	1.13E-08
log_sigmaPhi2_k	-0.30704	-Inf	-0.30704	Inf	-5.45E-09
log_sigmaPhi2_k	-0.50036	-Inf	-0.50036	Inf	-6.24E-10
log_sigmaPhi2_k	-0.35646	-Inf	-0.35646	Inf	-2.51E-09

Table 4-2 Continuing with the dataset for the period 2017-2022.

Parameter	Starting value	Lower boundary	Maximum likelihood estimation	Upper boundary	Final gradient
ln_H_input	-0.21131	-5	-0.21131	5	1.94E-05
ln_H_input	0.15809	-5	0.15809	5	-5.08E-05
beta1_ft_2017	0.85771	-Inf	0.85777	Inf	-6.92E-07
beta1_ft_2018	-0.10296	-Inf	-0.10307	Inf	-1.96E-06
beta1_ft_2019	-0.81324	-Inf	-0.81321	Inf	-1.42E-07
beta1_ft_2020	-0.47743	-Inf	-0.47735	Inf	-3.61E-06
beta1_ft_2021	0.75170	-Inf	0.75174	Inf	-4.61E-06
beta1_ft_2022	1.24197	-Inf	1.24191	Inf	1.23E-05
L_eta1_z	-0.68443	-Inf	-0.68442	Inf	-6.82E-06
L_omega1_z	1.32761	-Inf	1.32764	Inf	2.95E-06
L_epsilon1_z	0.89294	-Inf	0.89296	Inf	-3.24E-05
logkappa1	-2.92728	-4.766133	-2.92731	-1.174951	-2.75E-05
log_sigmaPhi1_k	-0.44992	-Inf	-0.44987	Inf	1.84E-06
log_sigmaPhi1_k	-0.06958	-Inf	-0.06956	Inf	-5.69E-07
log_sigmaPhi1_k	0.14800	-Inf	0.14803	Inf	3.83E-06
beta2_ft_2017	-2.98806	-Inf	-2.98804	Inf	-4.14E-07
beta2_ft_2018	-2.59742	-Inf	-2.59742	Inf	4.99E-06
beta2_ft_2019	-3.71074	-Inf	-3.71072	Inf	-6.22E-07
beta2_ft_2020	-3.67660	-Inf	-3.67671	Inf	-4.85E-07
beta2_ft_2021	-2.76986	-Inf	-2.76987	Inf	4.79E-06
beta2_ft_2022	-3.25114	-Inf	-3.25116	Inf	-8.65E-06
L_eta2_z	0.36590	-Inf	0.36589	Inf	-2.27E-06
L_omega2_z	0.26705	-Inf	0.26705	Inf	1.15E-06
L_epsilon2_z	-0.99996	-Inf	-0.99996	Inf	-7.79E-05
logkappa2	-2.19173	-4.766133	-2.19173	-1.174951	5.31E-05
log_sigmaPhi2_k	-0.07984	-Inf	-0.07984	Inf	2.18E-06
log_sigmaPhi2_k	-0.01947	-Inf	-0.01947	Inf	2.79E-06
log_sigmaPhi2_k	-0.30261	-Inf	-0.30261	Inf	-1.86E-05

Table 4-3 Continuing with the dataset without chartered vessels for the period 2017-2022.

Parameter	Starting value	Lower boundary	Maximum likelihood estimation	Upper boundary	Final gradient
ln_H_input	-0.25144	-5	-0.25145	5	-4.90E-08
ln_H_input	-0.01812	-5	-0.01812	5	2.62E-08
beta1_ft_2017	0.34008	-Inf	0.34021	Inf	-5.15E-09
beta1_ft_2018	-0.58870	-Inf	-0.58862	Inf	-5.52E-09
beta1_ft_2019	-1.21156	-Inf	-1.21149	Inf	-1.59E-09
beta1_ft_2020	-0.84933	-Inf	-0.84924	Inf	-4.56E-09
beta1_ft_2021	-0.33566	-Inf	-0.33562	Inf	2.63E-09
beta1_ft_2022	0.45257	-Inf	0.45265	Inf	-7.57E-10
L_eta1_z	0.86981	-Inf	0.86981	Inf	-3.66E-09
L_omega1_z	1.25162	-Inf	1.25164	Inf	-2.94E-08
L_epsilon1_z	-0.84051	-Inf	-0.84052	Inf	1.32E-08
logkappa1	-2.90937	-4.733377	-2.90940	-1.176148	-4.12E-08
log_sigmaPhi1_k	0.01885	-Inf	0.01889	Inf	-6.70E-09
log_sigmaPhi1_k	-0.12434	-Inf	-0.12433	Inf	-2.04E-09
log_sigmaPhi1_k	0.03804	-Inf	0.03805	Inf	-6.76E-08
beta2_ft_2017	-2.98338	-Inf	-2.98339	Inf	-8.93E-10
beta2_ft_2018	-2.69077	-Inf	-2.69076	Inf	-2.33E-10
beta2_ft_2019	-3.65369	-Inf	-3.65368	Inf	1.90E-09
beta2_ft_2020	-3.74236	-Inf	-3.74235	Inf	8.02E-09
beta2_ft_2021	-2.82328	-Inf	-2.82329	Inf	2.17E-10
beta2_ft_2022	-3.19590	-Inf	-3.19590	Inf	1.14E-10
L_eta2_z	0.34906	-Inf	0.34906	Inf	5.10E-09
L_omega2_z	-0.22239	-Inf	-0.22240	Inf	3.91E-09
L_epsilon2_z	1.00104	-Inf	1.00104	Inf	-1.91E-08
logkappa2	-2.20897	-4.733377	-2.20897	-1.176148	2.47E-08
log_sigmaPhi2_k	-0.18624	-Inf	-0.18623	Inf	-6.47E-09
log_sigmaPhi2_k	-0.14913	-Inf	-0.14913	Inf	-2.51E-09
log_sigmaPhi2_k	-0.32522	-Inf	-0.32521	Inf	1.74E-07

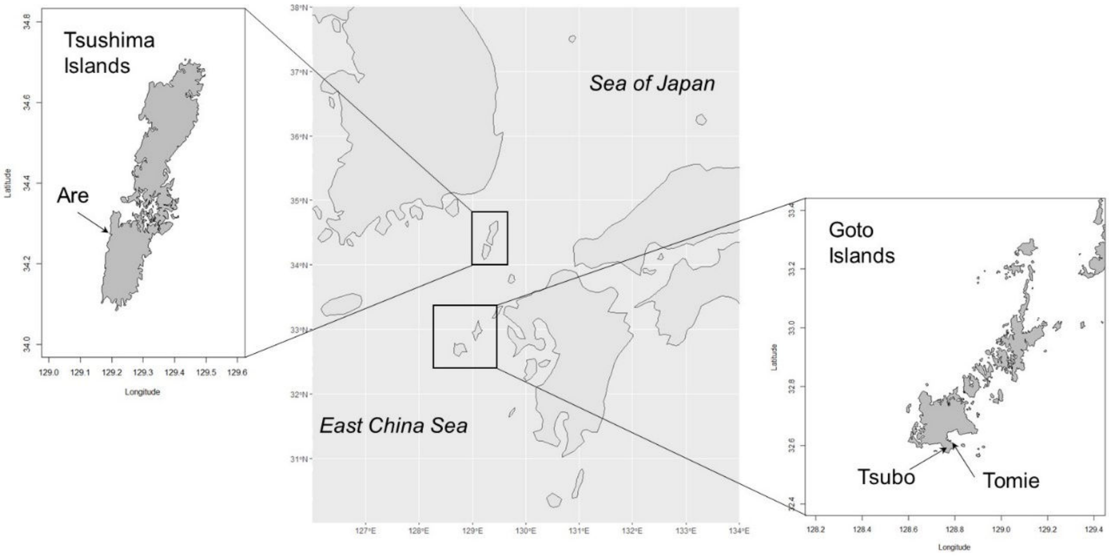

Figure 1 Location of fishing ports where real-time monitoring data of troll fisheries have been collected in Nagasaki prefecture. Left: 5 vessels in Izuhara-Are, Tsushima Islands. Right: 5 vessels in Goto-Tomie, and 4 vessels in Goto-Tsubo, Goto Islands.

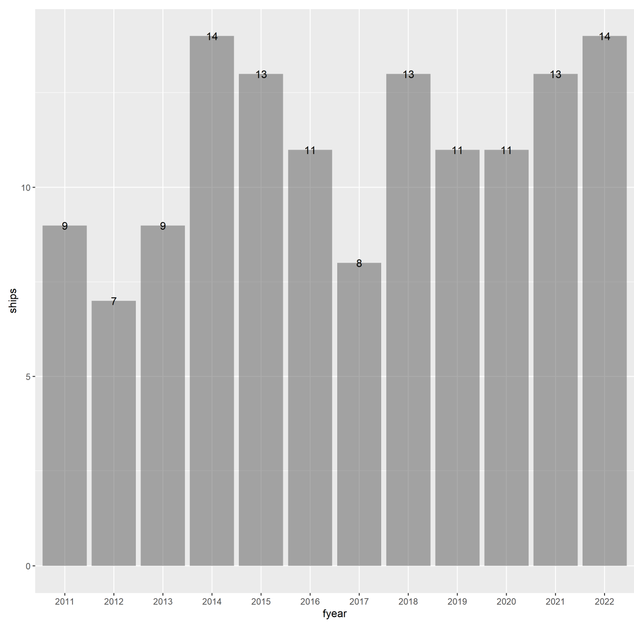

Figure 2 The number of real-time monitoring vessels with PBF operations from 2011 to 2022.

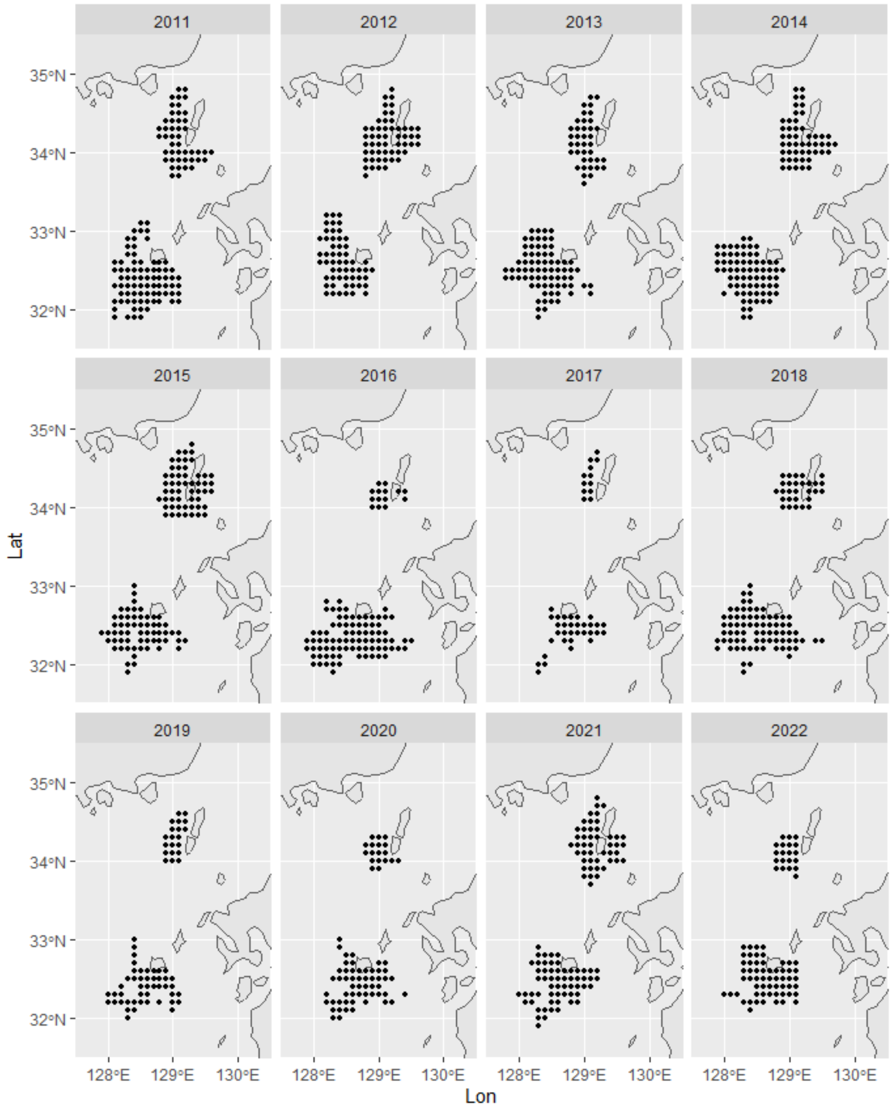

Figure 3 Distribution of troll operations of 7-14 real-time monitoring vessels from 2011 to 2022 fishing year for abundance estimation by the VAST model analysis. Data for the 2021-2022 fishing year includes chartered real-time monitoring in addition to conventional real-time monitoring as in 2011-2020.

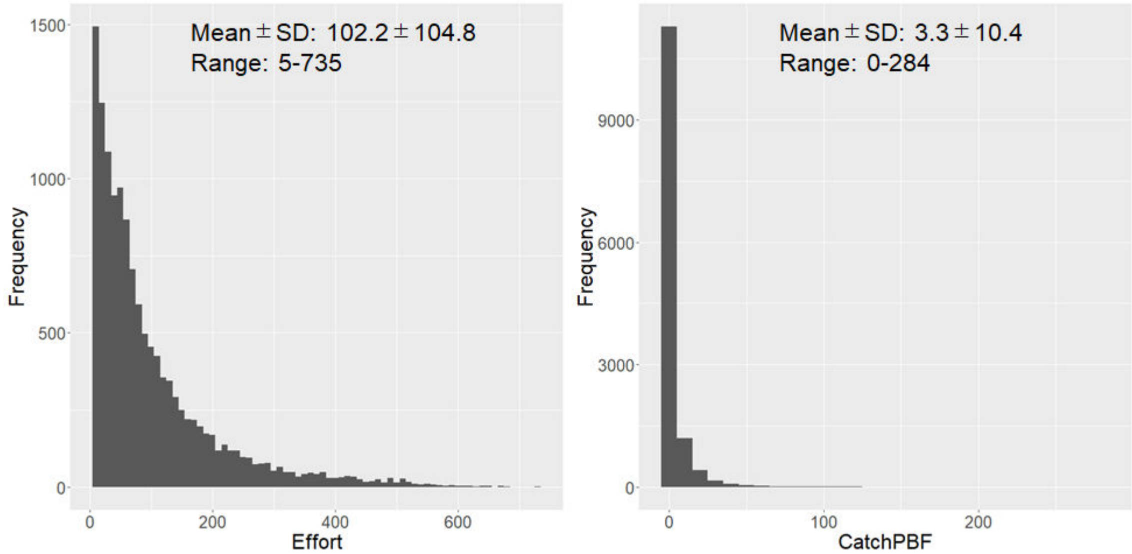

Figure 4 Frequency of fishing efforts (left) and PBF catches (right) for 2011-2022 based on 0.1 degree grid aggregate data.

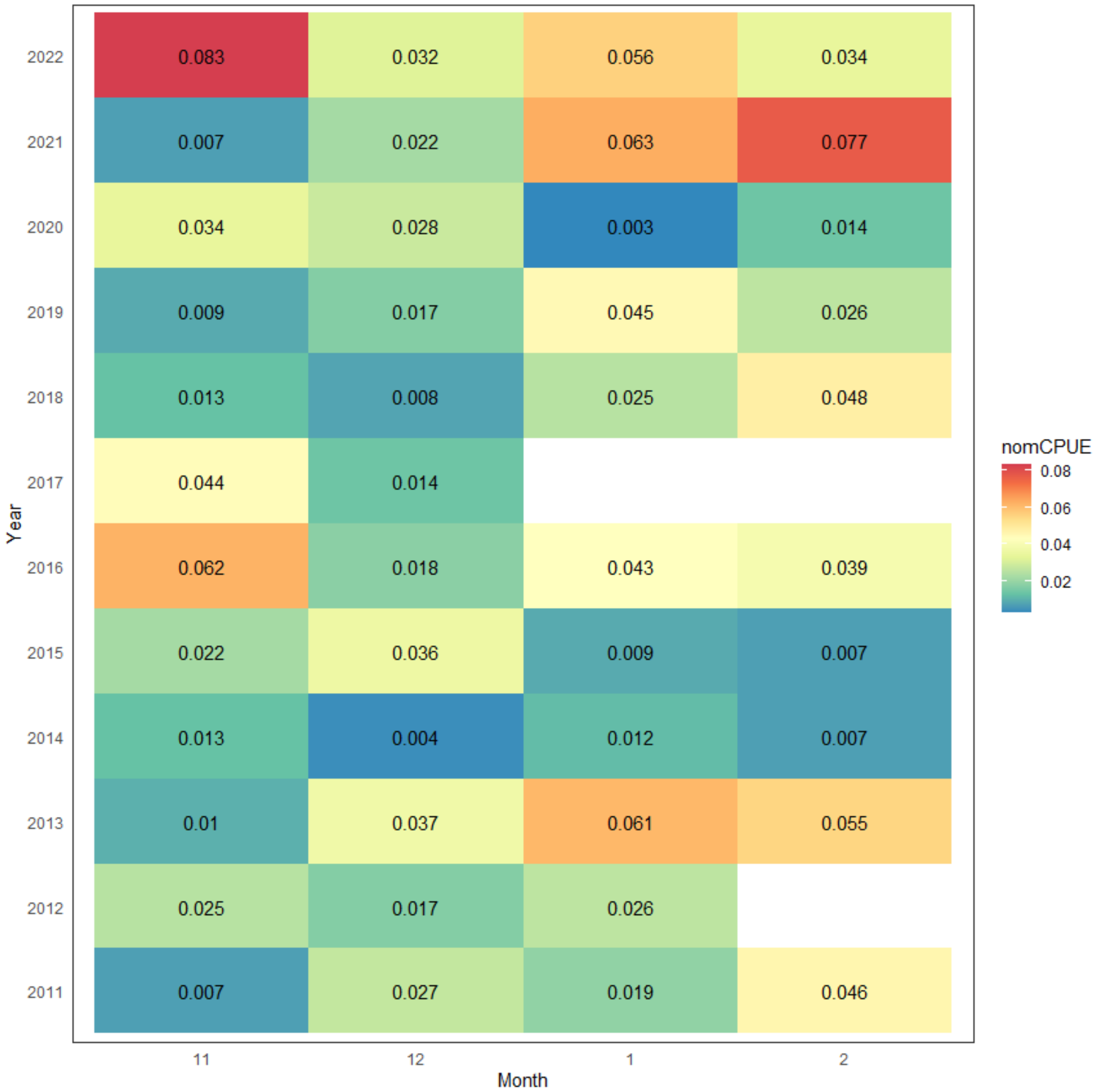

Figure 5 Nominal CPUE during 2011-2022 fishing year for each month (November to following February). No operations during the months of January and February of 2017 due to fishing regulations.

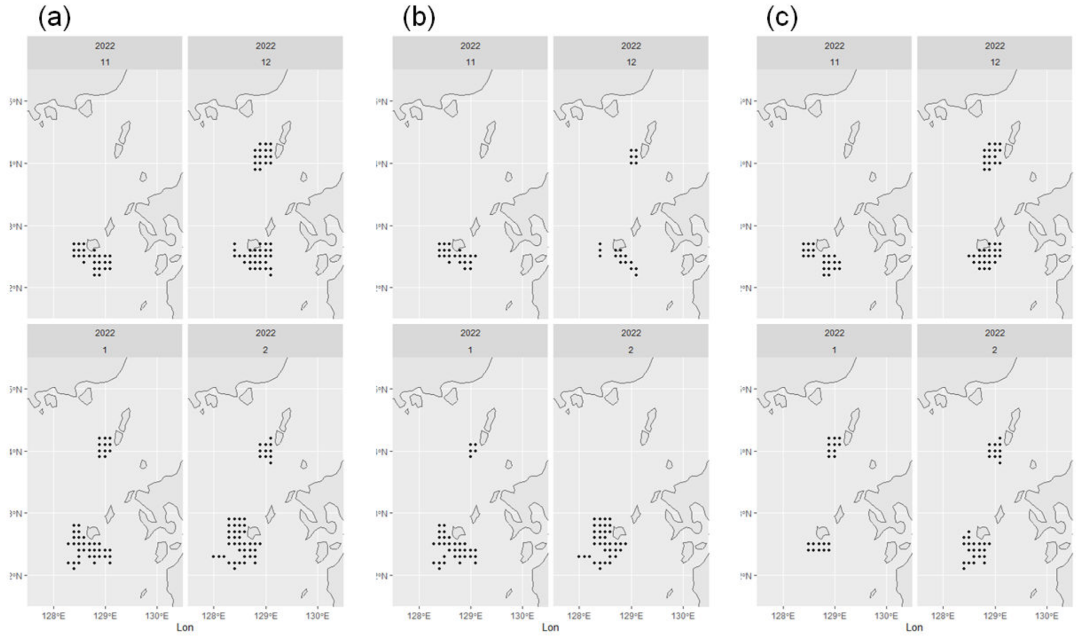

Figure 6 (a) Monthly spatial distribution of troll operations of 14 real-time monitoring vessels for the 2022 fishing year, and of these, (b) conventional real-time monitoring and (c) chartered real-time monitoring. Both monitoring surveys were conducted by the same 14 troll vessels. No charter operations around Tsushima in November due to delays in contract processing (*see* (c) top left).

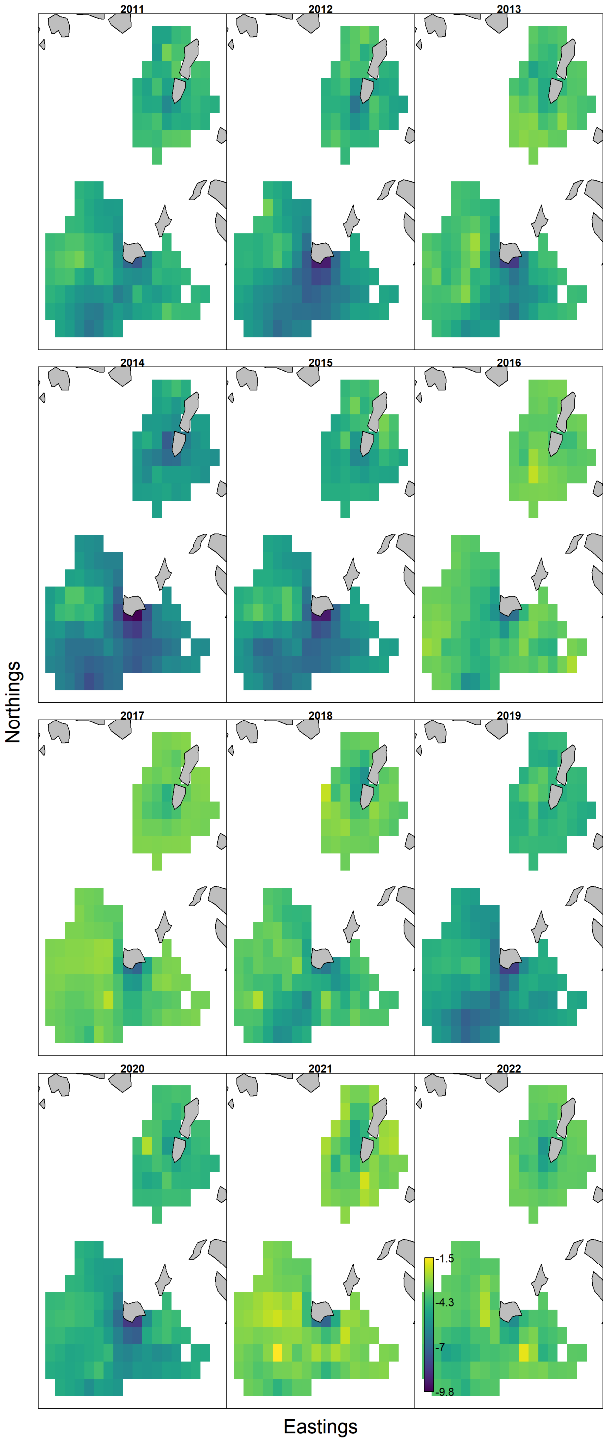

Figure 7-1 Spatio-temporal distribution of the log-transformed predicted densities of PBF for the 2011-2022 fishing year analyzed by VAST model. Warmer and cooler colors indicate high and low values, respectively.

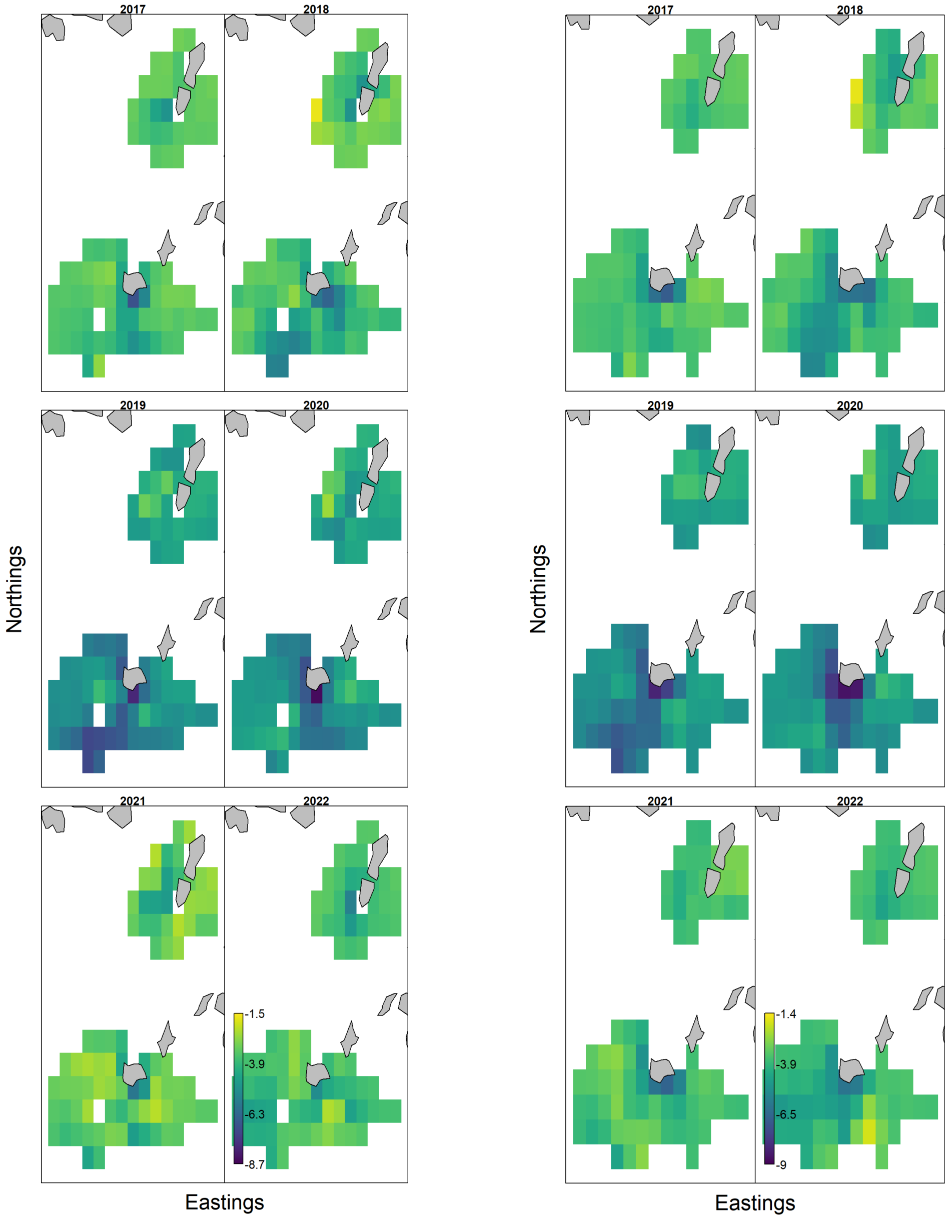

Figure 7-2 Continuing with the dataset for the period 2017-2022. Left: entire dataset. Right: without chartered monitoring dataset.

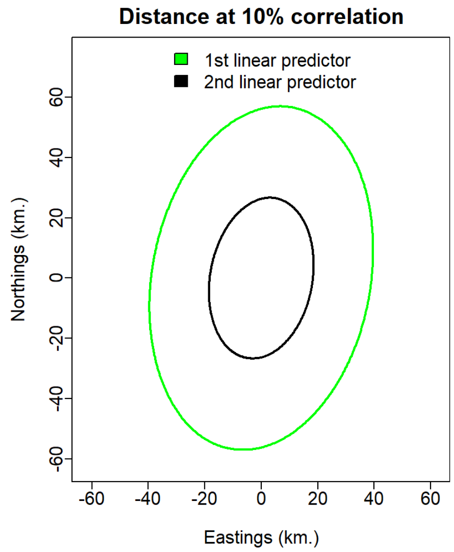

Figure 8-1 Decorrelation distance for different directions relative to encounter probability and positive catch rate for each of the two data periods 2011-2022. Indicating the magnitude of 2-dimensional spatial autocorrelation, and the ellipse signifies the distance (from a point located at position (0,0)), where the correlation drops to 10 %. The predicted densities correlated over a longer distance in the north-south direction than in the east-west direction.

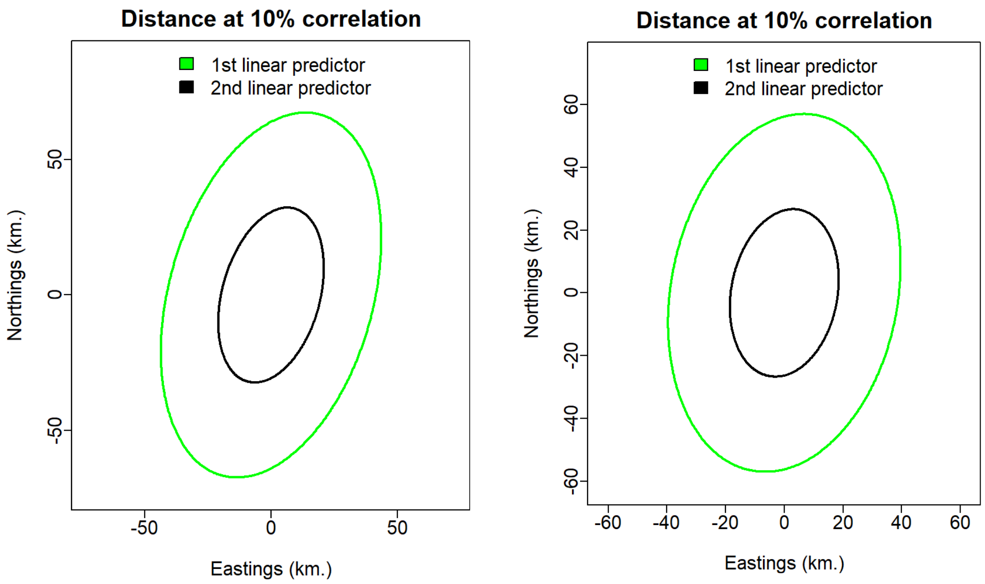

Figure 8-2 Continuing with the dataset for the period 2017-2022. Left: entire dataset. Right: without chartered monitoring dataset.

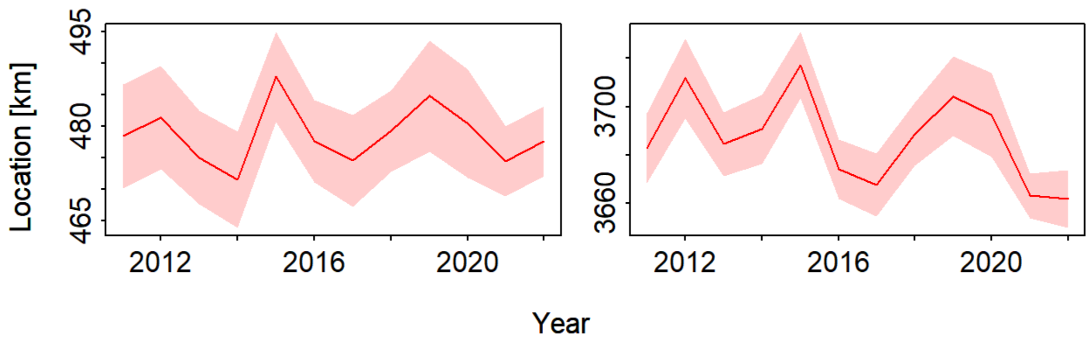

Figure 9-1 The center of gravity of PBF recruitments indicating the sift in distribution (distance (km)) in the east-west (left) and north-south (right) directions for the periods of 2017-2021. The thick line with shading indicates the mean value and standard error.

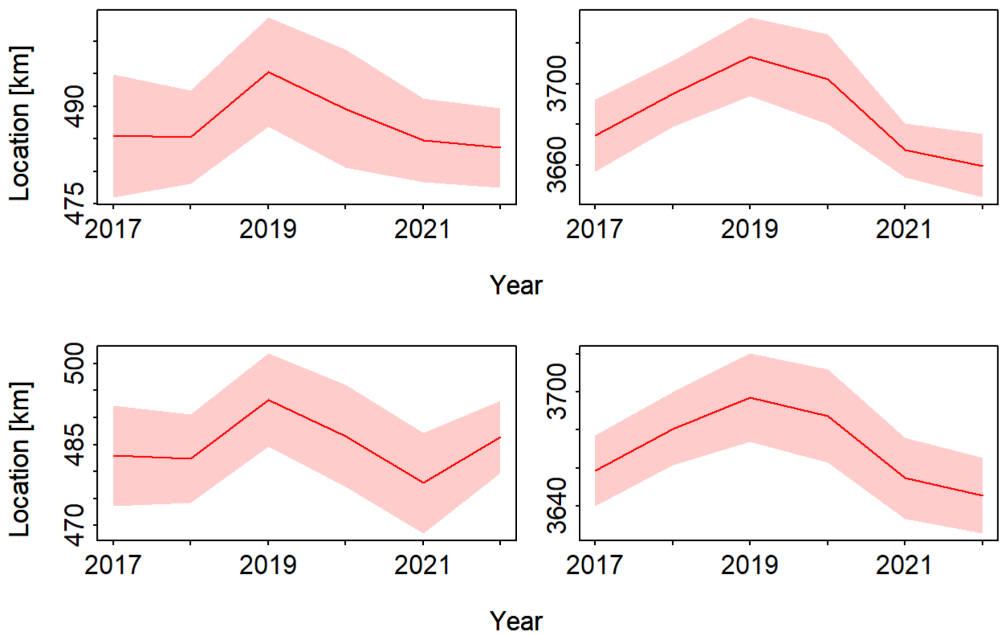

Figure 9-2 Continuing with the dataset for the period 2017-2022. Top: entire dataset. Bottom: without chartered monitoring dataset.

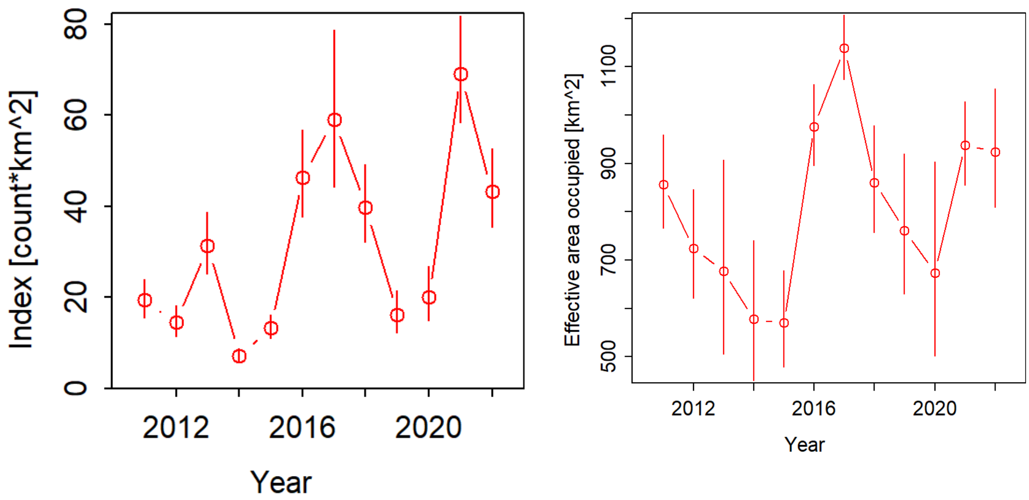

Figure 10-1 Standardized index of relative abundance of PBF (left) and estimated of the effective area occupied by PBF indicating range expansion/contraction (right) for the periods of 2011-2022. The open circles with vertical lines denote point estimates with standard errors.

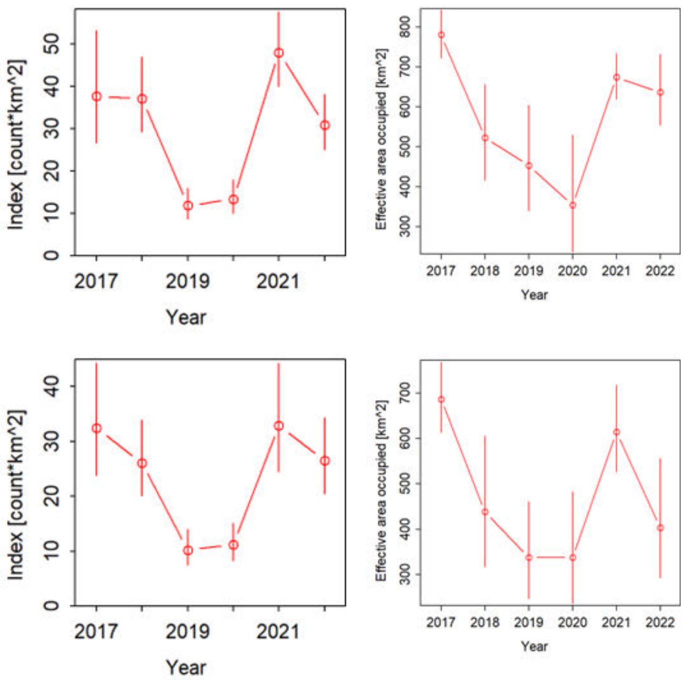

Figure 10-2 Continuing with the dataset for the period 2017-2022. Top: entire dataset. Bottom: without chartered monitoring dataset.

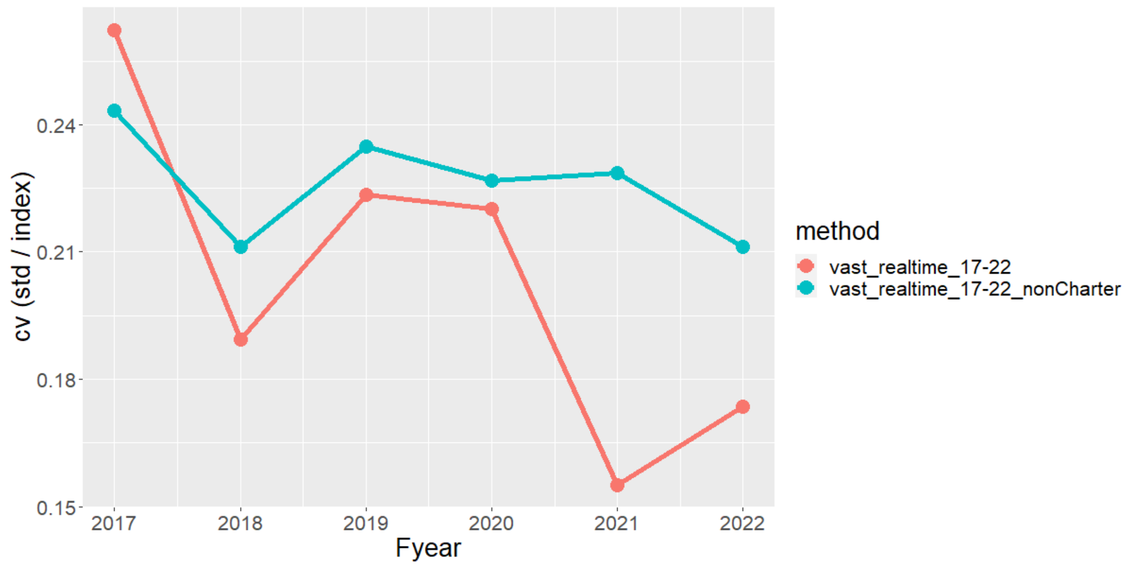

Figure 11 Comparison of coefficient of variation (CV) with (red line) and without (blue line) chartered real-time monitoring data from 2017 to 2022. CV was calculated that the standard deviation divided by the standardized index of relative abundance (*see* Fig. 10-2).

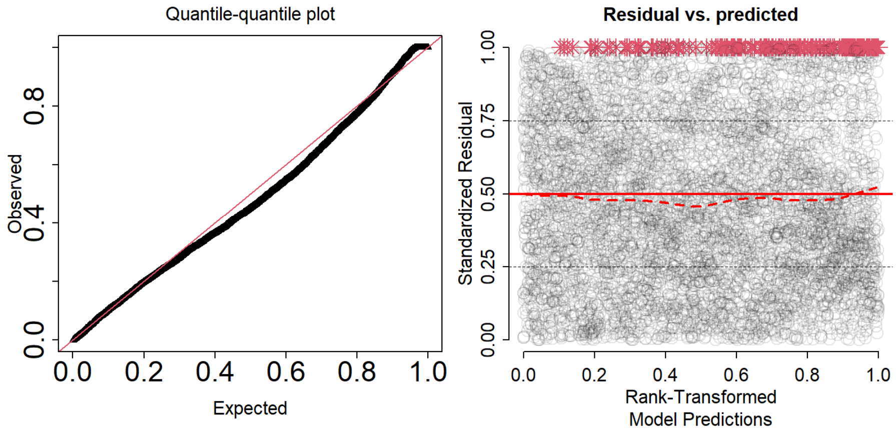

Figure 12-1 Diagnostic Q-Q plot (left) and residual plots (right) comparing the observed and predicted quantiles for the periods of 2011-2022. The residual plot calculating a quantile regression to compare the empirical 0.5 quantile in y-direction (dashed red lines) with the theoretical 0.5 quantile (red solid line).

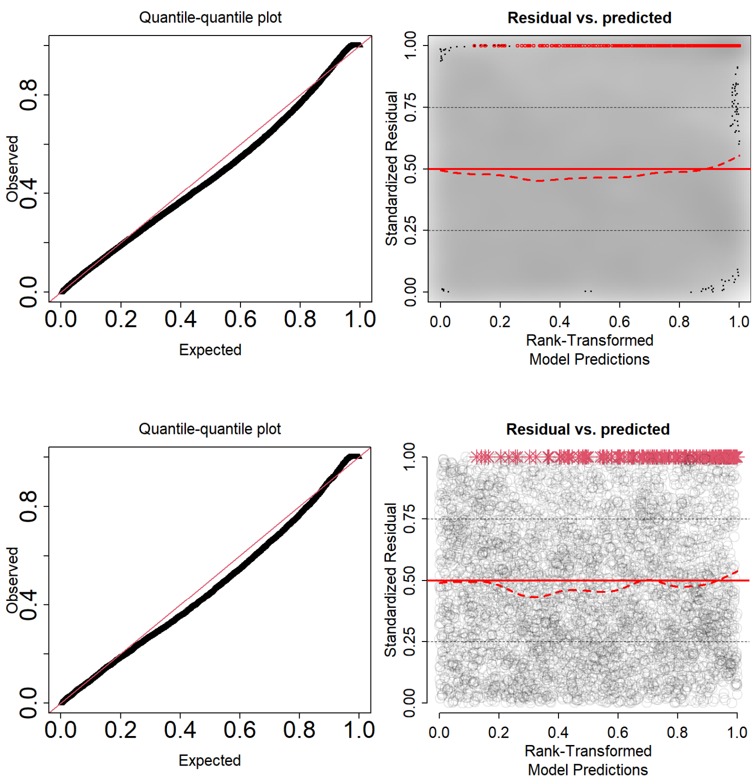

Figure 12-2 Continuing with the dataset for the period 2017-2022. Top: entire dataset. Bottom: without chartered monitoring dataset.

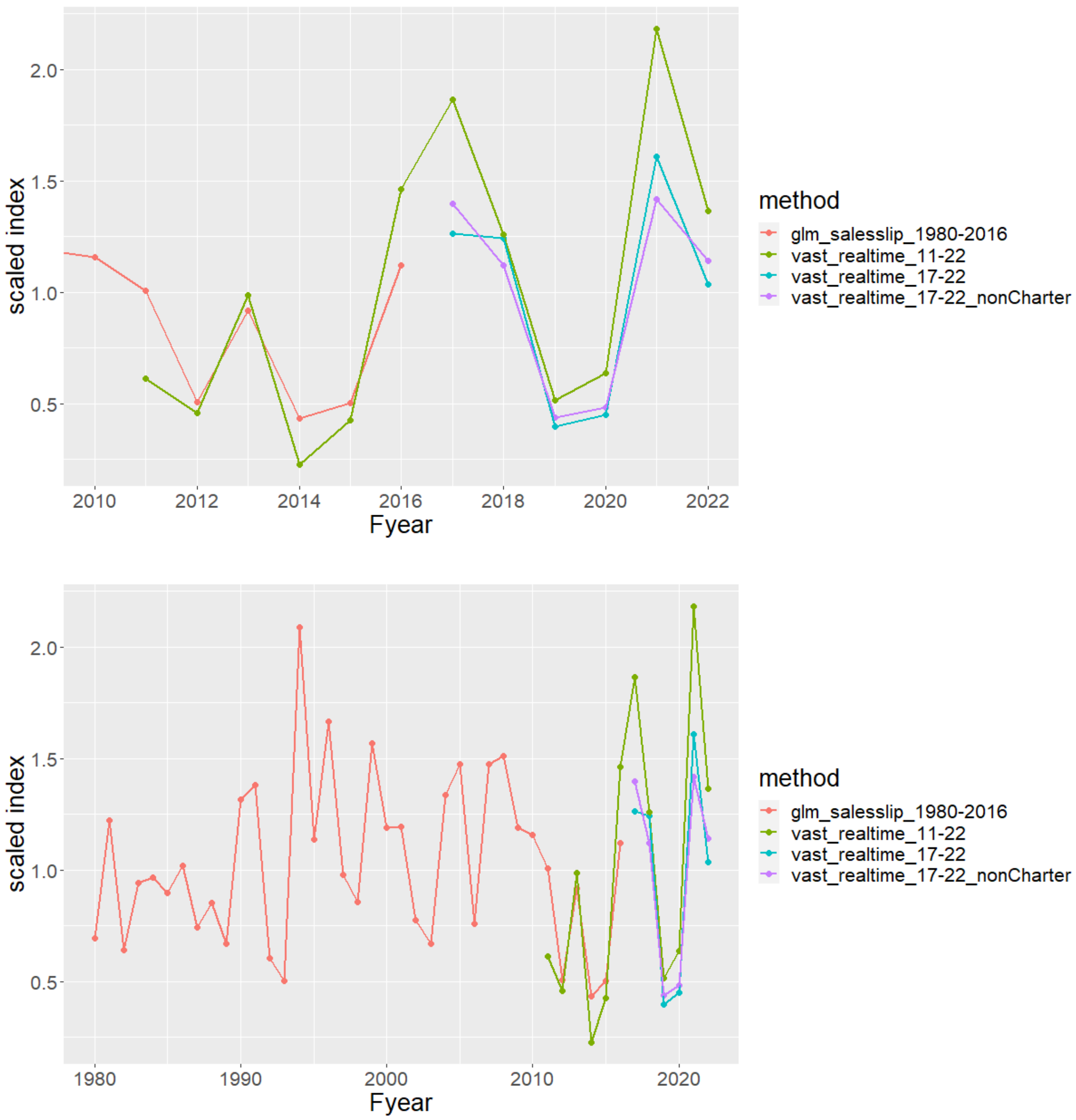

Figure 13 Recent trends of scaled abundance indices on results both traditional GLM (red line) using sales slip data (Nishikawa et al., 2021) and VAST analyses using real-time monitoring data for the periods 2011-2022 (green line) (top). For the period of 2017-2022, estimated index with (blue line) and without (purple line) chartered real-time monitoring data. Full time-series indices are shown in bottom figure.